

Constraint Handling of an Airbreathing Hypersonic Vehicle via Predictive Reference Management

Vincent Liu, Chris Manzie, and Peter M. Dower

Abstract—In this paper we consider the problem of constraint handling for an airbreathing hypersonic vehicle (HSV) through a hierarchical control architecture. A reference manager is incorporated as an intermediate control loop whose role is to modify an offline generated reference trajectory, without knowledge of disturbances, to enforce state and input constraints. Compared with traditional constraint handling approaches in HSV literature, this proposed approach allows for the deployment of controllers that are not typically formulated to handle constraints. We provide a computation time and constraint management comparison between a scheme that directly utilizes the nonlinear vehicle model and one that performs online linearization of the model.

I. INTRODUCTION

Pioneered by the North American X-15 program in 1954 [1], hypersonic flight continues to be an important area of aerospace research with applications in both the civilian and defense domains. To ensure viability in commercial and military applications, hypersonic vehicles (HSVs) need to be economic, reproducible, reliable, and safe [2]. A ramification of such design objectives is that these vehicles will operate at, or close to, design limits. This requires that the control system is equipped with constraint handling capabilities. Techniques such as barrier Lyapunov functions [3] and model predictive control [4] have been proposed to address system constraints.

In particular, predictive control approaches [5] have seen wide adoption in applications across a number of domains, especially when a linear time-invariant plant model is available. However, these formulations typically involve numerically solving an online optimization problem. This can be quite formidable especially considering the fast sampling times (typically a few milliseconds) required for sufficient control authority of HSVs, which is compounded by high model orders and severe nonlinearities. An alternative is the use of reference or command governors (RG/CG) [6], [7]. This approach acts as an augmentation to a system with an initial control design, the latter of which may not necessarily be able to handle system constraints. It modifies the incoming reference so that pointwise-in-time input and/or state constraints are satisfied and the modified reference is made as close to the desired reference as possible (see Figure 1). This sits between the reference signal and the closed-loop control

The authors are with the Department of Electrical and Electronic Engineering, The University of Melbourne, VIC, 3010 Australia (email: liuv2@student.unimelb.edu.au; manziec@unimelb.edu.au; pdower@unimelb.edu.au). This research was supported by the Australian Commonwealth Government through the Ingenium Scholarship and is part of a collaboration with BAE systems funded through an Australian Research Council Linkage Project grant (Grant number: LP190100104).

system, forming a hierarchical control architecture wherein the responsibility for constraint handling is delegated to the RG or CG and the controller is responsible only for providing stability and tracking performance. This reduces the online computational burden for the controller and since the closed-loop system is assumed to satisfy some notion of stability, the RG or CG can operate on slower sampling times.

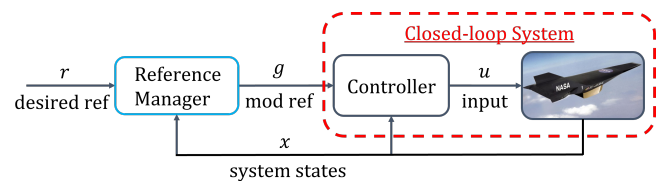


Fig. 1. Schematic diagram depicting the reference manager, which augments a standard feedback control loop.

The focus of this paper is to describe a framework in which input and state constraints can be enforced for generic vehicle models in aerospace applications involving control designs that ignore constraints. This framework will be demonstrated on a nonlinear HSV model with a feedback linearizing controller. Two approaches will be described and implemented including a reference governor for nonlinear systems [8] and a command governor for an online linearized system adapted from [7]. In the nonlinear approach, assumptions required for theoretic guarantees will be validated for a class of stabilising controllers. This is not afforded to online linearized models, but are nonetheless commonly used in this area due to their computational superiority. Although reference and command governors see some use in HSV literature [9], much of this work is solely applied to linearizations of the model and across relatively short trajectories. The framework we present is indifferent towards the system model, unlike tailored designs such as backstepping control [10], and requires only modest assumptions on the compensated closed-loop system.

II. SYSTEM MODEL

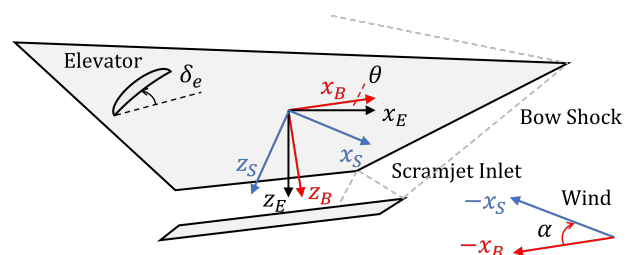


Fig. 2. Schematic diagram of an airbreathing hypersonic vehicle with labelled axes for the inertial E , stability S , and body B frame.

The airbreathing HSV model used in this paper is the control-oriented model found in [11]. The 5th-order rigid

body aircraft model is presented below with a visual of the required frames needed to understand the system states displayed in Figure 2.

$$\dot{h} = V \sin(\theta - \alpha), \quad (1a)$$

$$\dot{V} = \frac{1}{m} (T \cos(\alpha) - D) - a_g \sin(\theta - \alpha), \quad (1b)$$

$$\dot{\alpha} = \frac{1}{mV} (-T \sin(\alpha) - L) + Q + \frac{a_g}{V} \cos(\theta - \alpha), \quad (1c)$$

$$\dot{\theta} = Q, \quad \dot{Q} = \frac{1}{I_{yy}} M, \quad (1d)$$

where

- h is the altitude directed in the negative z_E -axis;
- V is the velocity along the positive x_S -axis;
- α is the angle-of-attack, which is the rotation of the body frame B relative to the stability frame S ;
- θ is the pitch angle, which is a rotation of the body frame B relative to the inertial frame E ;
- T, L, D, M is the thrust produced by the scramjet, the aerodynamic lift and drag, and the combined moment along the stability axes, respectively;
- I_{yy}, m, a_g is the moment of inertia, mass, and gravitational acceleration, respectively.

The forces and moments, whose functional dependencies have been omitted by abuse of notation for brevity, are given by the static maps in (2) and (3).

$$T = C_3^T(\phi)\alpha^3 + C_2^T(\phi)\alpha^2 + C_1^T(\phi)\alpha + C_0^T(\phi), \quad (2a)$$

$$L = \frac{1}{2}\rho V^2 \bar{S} (C_1^L \alpha + C_0^L), \quad (2b)$$

$$D = \frac{1}{2}\rho V^2 \bar{S} (C_2^D \alpha^2 + C_1^D \alpha + C_0^D), \quad (2c)$$

$$M = z^T T + \frac{1}{2}\rho V^2 \bar{S} \bar{c} C^M(\alpha, \delta_e), \quad (2d)$$

and

$$C_3^T(\phi) = \beta_1 \phi + \beta_2, \quad C_2^T(\phi) = \beta_3 \phi + \beta_4, \quad (3a)$$

$$C_1^T(\phi) = \beta_5 \phi + \beta_6, \quad C_0^T(\phi) = \beta_7 \phi + \beta_8, \quad (3b)$$

$$C^M(\alpha, \delta_e) = C_2^M \alpha^2 + C_1^M \alpha + C_e^M \delta_e + C_0^M, \quad (3c)$$

where

- \bar{S}, z^T, \bar{c} is the reference area, thrust moment arm and mean aerodynamic chord length, respectively;
- $\rho = \rho_0$ is the air density, assumed to be constant across the trajectory of interest;
- δ_e, ϕ is the elevator deflection and stoichiometrically normalised fuel-to-air ratio.

A second-order actuator model is incorporated for the input ϕ , which is given by

$$\ddot{\phi} = -2\zeta\omega\dot{\phi} - \omega^2\phi + \omega^2\phi_c \quad (4)$$

where ζ is the damping ratio, ω is the natural frequency and ϕ_c is the fuel-to-air ratio command. This augments the model in [11] and acts to increase model fidelity by simulating delays that would be experienced by the real system. From the perspective of control design, ϕ_c and δ_e are the new system inputs.

III. HYPERSONIC VEHICLE CONTROL DESIGN

To complete the closed-loop system in Figure 1, we require a controller to be designed for the HSV model in (1). Here we follow [11] and select an LQR controller designed for a feedback linearized HSV model [12]. To begin, we define the system state, input, and output vectors as follows

$$x = [V \quad \alpha \quad \theta \quad Q \quad \phi \quad \dot{\phi}]', \quad (5a)$$

$$u = [\delta_e \quad \phi_c]', \quad y = [V \quad \gamma]'. \quad (5b)$$

Substituting (2) into the HSV model in (1) and (4) generates a system model of the form

$$\dot{x}(t) = \mathcal{F}(x) + \mathcal{G}(x)u, \quad y = \mathcal{H}(x). \quad (6)$$

We now define the transformation of coordinates $\xi = \mathcal{T}(x) = [V \quad \dot{V} \quad \ddot{V} \quad \gamma \quad \dot{\gamma} \quad \ddot{\gamma}]'$ and the decoupling matrix is described using Lie derivative notation by

$$A(x) = \begin{bmatrix} L_{G_1} L_{\mathcal{F}}^2 \mathcal{H}_1(x) & L_{G_2} L_{\mathcal{F}}^2 \mathcal{H}_1(x) \\ L_{G_1} L_{\mathcal{F}}^2 \mathcal{H}_2(x) & L_{G_2} L_{\mathcal{F}}^2 \mathcal{H}_2(x) \end{bmatrix}. \quad (7)$$

Here \mathcal{H}_i corresponds to the i^{th} element of \mathcal{H} and \mathcal{G}_i corresponds the i^{th} column of \mathcal{G} . The feedback linearizing control law

$$u = A^{-1}(x) \left(\begin{bmatrix} v_1 \\ v_2 \end{bmatrix} - \begin{bmatrix} L_{\mathcal{F}}^3 \mathcal{H}_1(x) \\ L_{\mathcal{F}}^3 \mathcal{H}_2(x) \end{bmatrix} \right) \quad (8)$$

renders the system dynamics linear with respect to the new inputs v_1, v_2 and the state ξ . The system can then be described as

$$\ddot{V} = v_1, \quad \ddot{\gamma} = v_2. \quad (9)$$

Let $r \doteq [r^V \quad \dot{r}^V \quad \ddot{r}^V \quad r^\gamma \quad \dot{r}^\gamma \quad \ddot{r}^\gamma \quad \ddot{r}^{\gamma\gamma}]'$ denote the desired reference vector, where r^V, r^γ are the velocity and flight path angle references, respectively. The modified reference vector (see ‘‘mod ref’’ in Figure 1) is then denoted by $g \doteq [g_0^V \quad g_1^V \quad \dots \quad g_3^\gamma]'$, where g_i^j is the modified component corresponding to the i^{th} time derivative of r^j . With this, we construct the full-state feedback control law

$$v_1 = g_3^V - K^V [V - g_0^V \quad \dot{V} - g_1^V \quad \ddot{V} - g_2^V]', \quad (10a)$$

$$v_2 = g_3^\gamma - K^\gamma [\gamma - g_0^\gamma \quad \dot{\gamma} - g_1^\gamma \quad \ddot{\gamma} - g_2^\gamma]'. \quad (10b)$$

We compute the controller gains K^V, K^γ for the feedback linearized system in (9) using a standard LQR approach, leading to the controller gains

$$K^V = [10.0000 \quad 18.2674 \quad 11.6848], \quad (11a)$$

$$K^\gamma = [100.0000 \quad 174.1994 \quad 101.7271]. \quad (11b)$$

This controller will be emulated at a sampling period of 1 ms. To reduce errors due to floating-point arithmetic, (1) can be rescaled to measure altitude and velocity in units of 10^6 ft (or $\text{ft}\cdot\text{s}^{-1}$), and is done so here. A closed-loop system description, which is necessary for the RG and CG algorithms, can be obtained by substituting (10) and (8) in (6).

IV. REFERENCE GOVERNOR FOR NONLINEAR SYSTEMS

In this section we briefly review the relevant background and the key results and assumptions required for the RG in [8]. We then provide sufficient conditions that satisfy these assumptions for a general closed-loop system, which also hold for the HSV model in Section II with the feedback linearizing controller in Section III.

A. Background Theory [8]

Consider the continuous-time nonlinear system and constraint

$$\dot{x}(t) = f(x(t), g(t)), \quad x(0) = x_0, \quad (12a)$$

$$(x(t), g(t)) \in \mathcal{N}, \quad \forall t \geq 0, \quad (12b)$$

where $x(t) \in \mathbb{R}^n$ is the state vector, $g(t) \in \mathbb{R}^p$ is the modified reference vector at time t , $f : \mathbb{R}^n \times \mathbb{R}^p \rightarrow \mathbb{R}^n$ is a continuous function describing the closed-loop system dynamics, and $\mathcal{N} \subset \mathbb{R}^n \times \mathbb{R}^p$ is the constraint set. Additionally, we denote the solution of (12a) at time t to a constant reference $g(\cdot) \equiv \bar{g}$ with initial state $x(0) = x_0$ as $\mathcal{X}(t, x_0, \bar{g})$. The modified reference is described in discrete time by

$$g[k] = g[k-1] + \kappa[k](r[k] - g[k-1]), \quad (13)$$

where $r[k] \doteq r(k\Delta)$, with sampling period Δ , is the desired reference, $g[k]$ is assumed to be zero-order held across each sample, and $\kappa[k] \in [0, 1], \forall k \in \{0, 1, \dots\}$ is the interpolating factor. The goal of the RG is to make g as close to r as possible, subject to system constraints.

Next, we introduce the assumptions required to state the key results of [8]. The constraint set \mathcal{N} is defined by

$$\mathcal{N} \doteq \{(x, r) | n_q(x, r) \leq 0, \forall q \in \mathcal{Q} \doteq \{1, \dots, q_0\}\}. \quad (14)$$

in which $n_q : \mathbb{R}^n \times \mathcal{S} \rightarrow \mathbb{R}$, with $\mathcal{S} \subset \mathbb{R}^p$, are functions satisfying the following assumptions:

Assumption 1. \mathcal{N} is bounded;

Assumption 2. The functions n_q are continuous $\forall q \in \mathcal{Q}$;

Assumption 3. The set \mathcal{S} is compact and convex;

Assumption 4. $\exists \epsilon_0 > 0, t_0 \geq 0$ s.t $n_q(\mathcal{X}(t, x, r), r) \leq -\epsilon_0$ for all $t \geq t_0, q \in \mathcal{Q}, r \in \mathcal{S}$, and $(x, r) \in \mathcal{N}$.

We now define the continuous function $\Gamma \in C(\tilde{\mathcal{N}}, \mathbb{R})$ with $\tilde{\mathcal{N}} \doteq \mathcal{N} \cap (\mathbb{R}^n \times \mathcal{S})$ by

$$\Gamma(x, r) = \max\{n_q(\mathcal{X}(t, x, r), r) : q \in \mathcal{Q}, 0 \leq t \leq t_0\},$$

which is a compact set from Assumptions 1 to 3. Simply stated, the system (12a) is simulated from an initial state x with $g(\cdot) \equiv r$. The largest value $n_q(\mathcal{X}(t, x, r), r)$ for all $q \in \mathcal{Q}$ and $t \in [0, t_0]$ is then recorded as $\Gamma(x, r)$.

Finally, we select the interpolating factor $\kappa[k] \in [0, 1]$ as per [8] to be

$$\kappa[k] \doteq K(x[k], r[k], g[k-1]), \quad (15)$$

$$K(x, r, g) \doteq \begin{cases} \lambda^*, & \text{if } \lambda^* \|r - g\| \geq \delta \\ & \text{or } \Gamma(x, g) \leq -\epsilon, \\ 0, & \text{otherwise,} \end{cases} \quad (16)$$

with $\lambda^* \doteq \max\{\lambda \in [0, 1] : \Gamma(x, g + \lambda(r - g)) \leq 0\}$ and $\delta > 0, \epsilon > 0$ are fixed a priori.

Theorem 1. [8] Suppose Assumptions 1 to 4 hold, and there exists a $g^* \in \mathcal{S}$ such that $\Gamma(x_0, g^*) \leq 0$ and $r(t) \in \mathcal{S}$ for all $t \geq 0$, then if κ is computed according to (15) and $g(0) = g^*$ we have $g(t) \in \mathcal{S}$ and $(x(t), g(t)) \in \mathcal{N}$ for all $t \geq 0$. Moreover, for fixed constants $r_f \in \mathcal{S}$ and $t_f \in \mathbb{R}$, if $r(t) = r_f \forall t \geq t_f$, then there exists $\hat{t} \geq t_f$ such that $g(t) = r_f, \forall t \geq \hat{t}$.

Theorem 1 ensures solutions of (12a) are constraint admissible and g converges to any constant reference $r \in \mathcal{S}$. Note that other characterisations of Γ are possible (see [8]).

B. Sufficient Conditions for Assumptions 1 to 4

We now consider a special class of systems described by (12) that satisfy Assumptions 1 to 4.

Proposition 1. For a given $r \in \mathbb{R}^p$, let x_r be a unique equilibrium of (12a) with $g(t) \equiv r$. Suppose Assumptions 1 and 2 hold. Define \mathcal{S}_ϵ below, which is the set of references corresponding to constraint-admissible equilibria

$$\mathcal{S}_\epsilon \doteq \{r \in \mathbb{R}^p : n_q(x_r, r) \leq -\epsilon, \forall q \in \mathcal{Q}\}. \quad (17)$$

If there exists an $\epsilon_r > 0$ such that \mathcal{S}_{ϵ_r} has a non-empty interior, and x_r is globally attractive¹ for all $r \in \mathbb{R}^p$, then Assumptions 1 to 4 are satisfied.

Proof. Assumption 3 holds by taking \mathcal{S} to be a compact, convex subset of \mathcal{S}_{ϵ_r} , whose existence is implied by the non-empty interior of \mathcal{S}_{ϵ_r} . Since n_q are continuous functions, for any $\epsilon_r - \epsilon_0 > 0$ and $q \in \mathcal{Q}$ there exists an $\epsilon_q > 0$ such that $|n_q(\mathcal{X}(t, x, r), r) - n_q(x_r, r)| < \epsilon_r - \epsilon_0$ whenever $\|\mathcal{X}(t, x, r) - x_r\| < \epsilon_q$. Since x_r is globally attractive, for a given $r \in \mathcal{S}$ there exists a $T_r \geq 0$ such that for all $t \geq T_r$ we have $\|\mathcal{X}(t, x, r) - x_r\| < \epsilon$, where $\epsilon \doteq \min_{q \in \mathcal{Q}} \{\epsilon_q\}$. Thus, we have $\forall t \geq t_0 \doteq \max_{r \in \mathcal{S}} \{T_r\}, \forall r \in \mathcal{S}$, and $\forall q \in \mathcal{Q}$ the result $n_q(\mathcal{X}(t, x, r), r) < \epsilon_r - \epsilon_0 + n_q(x_r, r) \leq -\epsilon_0$, which means Assumption 4 holds. ■

It can be easily verified that the assumptions of Proposition 1 hold for the HSV model using the controller in Section III, so long as \mathcal{N} is not overly restrictive. Denote by ξ_r the asymptotically stable equilibrium of (9) with the control law in (10) to a constant reference $g(t) \equiv r$. Following (6), the map $\mathcal{T} : \mathbb{R}^n \rightarrow \mathbb{R}^n$ is continuous and invertible within operating regions of interest, which means $x_r \doteq \mathcal{T}^{-1}(\xi_r)$ is a unique, attractive equilibrium. Note that an arbitrarily large box constraint can be imposed to ensure boundedness of \mathcal{N} .

C. Algorithm Summary and Practical Implementation

The synthesis of the RG is summarised in Algorithm 1, which is evaluated at each time step k . Evaluating $\Gamma(x, r)$ in Algorithm 1 requires the forward simulation of the continuous-time system in (12a). A variety of routines in MATLAB exist for this, including ode45 and ode23s.

¹An equilibrium x_r is said to be globally attractive if for any $\epsilon > 0$ there exists a $T_r \geq 0$ such that $\|\mathcal{X}(t, x, r) - x_r\| < \epsilon$ for all $t \geq T_r$ and x such that $\|x - x_r\| \leq \Delta$, where Δ can be arbitrarily large.

Algorithm 1 Nonlinear Reference Governor Algorithm

1: **inputs**

The current state $x = x[k]$, the previous modified reference $g = g[k - 1]$, the desired reference $r = r[k]$, the function $\Gamma(x, r)$ and the tolerances δ, ϵ

2: **compute**

κ according to (15) and (16).

3: **return** κ

Remark 1. An approximate means of computing λ^* is given in Algorithm K of [8], which reduces the number of evaluations of $\Gamma(x, r)$.

Remark 2. Although it is possible to adapt the algorithm given in [13] to compute t_0 , this can be computationally formidable even for relatively simple systems. Instead, it suffices to obtain a fixed over-estimate of t_0 offline by simulating (12a) for a subset of $\tilde{\mathcal{N}}$ covering the expected operating conditions.

V. COMMAND GOVERNOR WITH ONLINE LINEARIZATION

A key limitation of the RG considered in the previous section is the computational cost associated with the forward simulation of the nonlinear system. This is already addressed in some sense as the search space of possible references $g[k]$ at time k is reduced to a line segment between $g[k - 1]$ and $r[k]$. However, if governing action is required for any component of $r[k]$, then all components are affected, which leads to sub-optimal behaviour in the sense that the Euclidean distance between $r[k]$ and $g[k]$ is made larger than necessary.

We now move to introducing an alternative implementation for a general nonlinear system which involves modifying the algorithms of [7] so that they are appropriate for an online linearized model. Since significant modifications are made, we omit the theoretical results of the original algorithm.

We first discuss the notation and preliminary system transformation steps required to understand the algorithm. Consider again the continuous-time nonlinear system in (12a). Augment (12a) with a continuous output map $h_c : \mathbb{R}^n \times \mathbb{R}^p \rightarrow \mathbb{R}$, yielding the corresponding output trajectory

$$c(t) = h_c(x(t), g(t)). \quad (18)$$

This output will be used as an alternative way to describe (12b).

Performing a linearization of (12a) and (18) about a point (\bar{x}, \bar{g}) and subsequently discretizing it with sampling period Δ by assuming a zero-order held reference g (see [14]) leads to a discrete-time affine model of the form

$$\tilde{x}[k + 1] = \Phi \tilde{x}[k] + G \tilde{g}[k] + f_0, \quad (19a)$$

$$c[k] = H \tilde{x}[k] + D \tilde{g}[k] + h_0, \quad (19b)$$

where $\tilde{x}[k] \doteq x[k] - \bar{x}$, $\tilde{g}[k] \doteq g[k] - \bar{g}$ are the perturbations.

The role of the command governor is to select $\tilde{g}[k]$ to enforce the constraint $c[k] \in \mathcal{C}$, $\forall k \geq 0$, where $\mathcal{C} \subset \mathbb{R}^{n_c}$. To

this extent, consider the following dynamic model for $\tilde{g}[k]$

$$\tilde{g}[k] = \mu[k] + w[k], \quad (20a)$$

$$\mu[k + 1] = \gamma \mu[k], \quad \gamma \in [0, 1), \quad (20b)$$

$$w[k + 1] = w[k], \quad (20c)$$

where $\mu[k] \in \mathbb{R}^p$ is the transient portion of $\tilde{g}[k]$ with $\gamma \in \mathbb{R}$ being a design parameter and $w[k] \in \mathbb{R}^p$ is the steady-state portion. At each sample time k , given the current state $\tilde{x}[k]$, the previous modified reference $\tilde{g}[k - 1]$, and the current desired reference $\tilde{r}[k]$, the following convex optimization problem is solved for the dynamics in (19) and (20).

$$\begin{bmatrix} \mu^* \\ w^* \end{bmatrix} = \arg \min_{\mu \in \mathbb{R}^p, w \in \mathbb{R}^p} \|\mu\|_{\Psi_\mu}^2 + \|w - \tilde{r}[k]\|_{\Psi_w}^2 + \|\mu + w - \tilde{g}[k - 1]\|_{\Psi_\delta}^2 \quad (21)$$

subject to $\mathcal{C}(\tilde{x}[k], \mu, w, i) \in \mathcal{C}$, $\forall i \in \{0, \dots, c_0\}$

where

- $\|x\|_{\Psi_\star}^2 \doteq x^T \Psi_\star x$ with $\Psi_\mu, \Psi_w, \Psi_\delta$ being symmetric positive definite matrices, which are design parameters;
- $\mathcal{C}(x, \mu, w, i)$ denotes the output sequence $\{c[k]\}$ in (19b) at time i from the initial state and reference $(\tilde{x}[0], \tilde{g}[0]) = (x, \mu + w)$;
- and $c_0 \in \mathbb{N} \cup \{0\}$ is a design parameter.

Algorithm 2 Modified Command Governor Algorithm

1: **inputs**

The current state $\bar{x} = x[k]$, the previous modified reference $\bar{g} = \tilde{g}[k - 1] + \bar{g}[k - 1]$, the desired reference $r = r[k]$, and the design parameters $\Psi_\mu, \Psi_w, \Psi_\delta, c_0$.

2: **compute**

the discrete-time model in (19) by performing a linearization of (12a) about (\bar{x}, \bar{g}) and subsequently discretizing the model using a sampling period Δ .

3: **solve**

the optimization problem in (21) with $\tilde{x} = x[k] - \bar{x}$, $\tilde{g} = \tilde{g}[k - 1]$, and $\tilde{r} = r - \bar{g}$.

4: **if** a feasible solution to (21) is found **then**

5: $\mu[k] \leftarrow \mu^*$, $w[k] \leftarrow w^*$, $\bar{g}[k] \leftarrow \bar{g}$

6: **else**

7: $\mu[k] \leftarrow \gamma \mu[k - 1]$, $w[k] \leftarrow w[k - 1]$, $\bar{g}[k] \leftarrow \bar{g}[k - 1]$

8: **return** $g[k] = \mu[k] + w[k] + \bar{g}[k]$

This formulation differs from [7] in that c_0 is not computed via an algorithm and there are no steady-state constraints or costs in (21). In [7], the algorithm used to compute c_0 for a stable, linear system can result in long prediction horizons. However, the linearized model may not hold across such a horizon, and selecting a shorter c_0 may help prevent ill-predicted constraint violations. The trade-off is that a short horizon may cause the CG to be unaware of future constraint violations, leading to infeasibility when solving (21). Similarly, steady-state behaviour is ill-predicted by models derived through linearization, so these have been omitted. When the constraint set can be described by linear inequalities, (21) becomes a quadratic program (QP).

Finally, the synthesis of the CG is summarised in Algorithm 2, which is computed at each time step k . A case describing the governing action when (21) is infeasible is included in lines 6-7, which is not presented in [7]. In this case, the reference evolves according to a sequence that was determined to be feasible at a previous time-step and ensures that $g[k]$ remains bounded when infeasibility occurs. If the HSV is equipped with a stabilising controller, feasibility is eventually recovered if the equilibrium associated with the constant reference $g[k] \equiv w + \bar{g}$ is constraint admissible.

VI. RESULTS AND EVALUATIONS

We now implement the reference and command governors on the nominal closed-loop HSV model with the feedback linearizing controller described in Section III. Appropriate system model parameters and RG /CG design parameters are given in Table I and Table II of the Appendix, respectively. The role of the RG and CG will be to enforce a fuel-to-air ratio constraint $0 \leq \phi \leq 0.55$ along the reference trajectory (r^V, r^γ) given in [11]. Simulations were performed in Simulink using the variable step integration method ode23s with a maximum step size of $40 \mu\text{s}$.

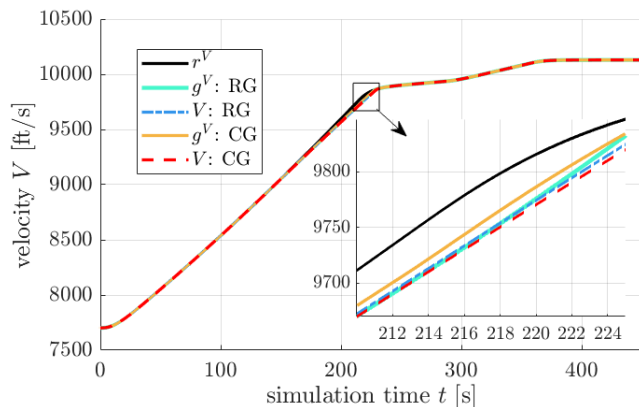


Fig. 3. Comparison of velocity tracking performance with a nonlinear reference governor (RG) and a modified command governor (CG).

Illustrative behaviours of the nonlinear RG and modified CG are presented in Figure 3 and 4 with the fuel-to-air ratio ϕ displayed in Figure 5. We first observe that both algorithms are able to successfully enforce the fuel-to-air ratio constraints, with reference/command governing action occurring around the interval $145 \leq t \leq 230$. A reduction in the slope of the velocity reference is necessary as ϕ is solely responsible for thrust production and thus controls the acceleration of the HSV. Although the CG produces a modified reference g^V that is closer to r^V , the velocity is almost identical, which corresponds to an almost identical fuel-to-air ratio command. This difference is likely due to the governing action that occurs on higher-order derivatives of the velocity reference, which are not displayed. Notice in Figure 4 that the nonlinear RG unnecessarily performs governing action on the flight path angle, which is not seen in the CG implementation. This is a consequence of the linear interpolation that is performed for the RG, whereas the CG is able to adjust individual components of the reference. We observe that ϕ departs slightly from its maximum operating

point in the interval $180 \leq t \leq 220$ for the CG. Such behaviour can likely be attributed to linearization errors that are not present in the RG, which directly utilizes the nonlinear model. However, its effect on the vehicle velocity is negligible.

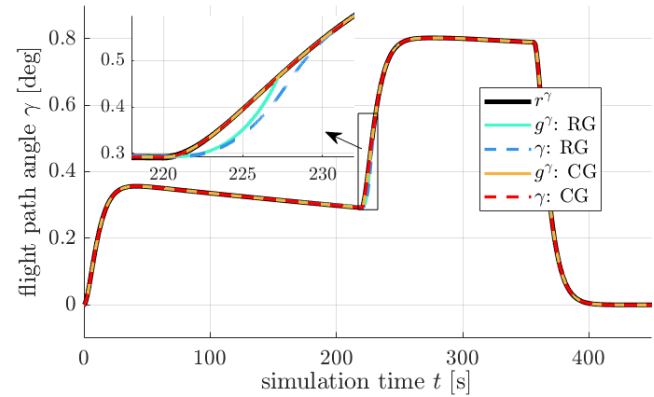


Fig. 4. Comparison of flight path angle tracking performance with a nonlinear reference governor (RG) and a modified command governor (CG).

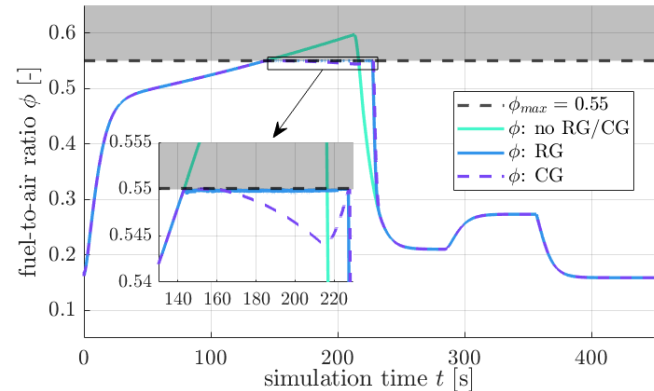


Fig. 5. Comparison of the fuel-to-air ratio ϕ and its upper constraint ϕ_{max} without governing action (no RG/CG), with the nonlinear reference governor (RG), and with the modified command governor (CG).

Using a four-core Intel® Core™ i7-1065G7 CPU, computation times with unoptimized code in MATLAB for the RG and CG are displayed in Figure 6. The median computation times are 23.11 ms and 5.18 ms with the 99th percentile being 97.39 ms and 12.64 ms for the RG and CG, respectively. We observe that the nonlinear RG requires more expensive updates, particularly when it comes to the worst case computation times. A potential remedy is to simply update the RG less frequently. However, from the perspective of the inner-loop controller, slow updates lead to large step-like changes in g , which can excite undesirable transient behaviour, see Figure 7. Moreover, slower updates lead to larger distances $\|r - g\|$. This is evidenced in the maximum altitude error $\|r^h - h\|_\infty$, which was 57.16 ft and 75.52 ft for the RG with $\Delta = 20$ ms and 200 ms, respectively. Note that the CG had an altitude error of only 13.71 ft, which is largely due to the lack of governing action required for the flight path angle.

Although the RG applied directly to the nonlinear HSV model enjoys theoretic guarantees, such benefits are diminished by the approximations required to implement it (see Remarks 1 and 2) as well as the online computational costs.

Additionally, some military applications may require high maneuverability, which is hindered by the unnecessary governing action performed by the nonlinear RG. In a practical setting, linearization-based strategies, such as the modified CG, may be more desirable as they offer a high performing alternative with improved update speeds.

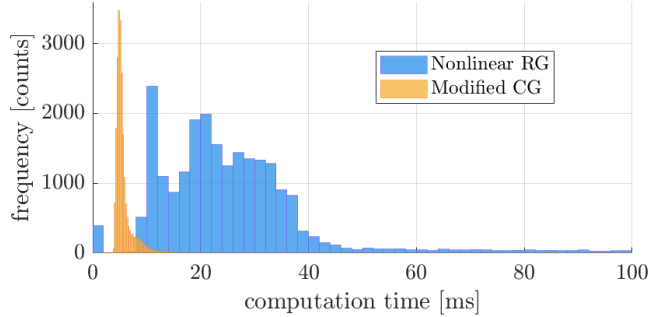


Fig. 6. Comparison of computation times for each update of the nonlinear reference governor and modified command governor as a histogram.

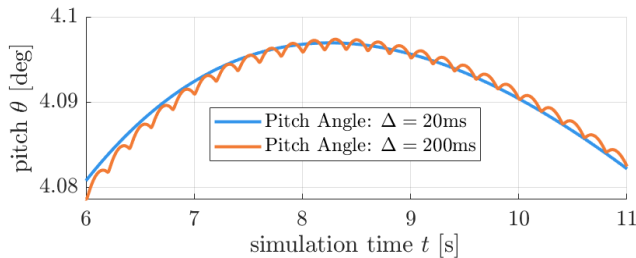


Fig. 7. Comparison of pitch angle for the nonlinear reference governor for two significantly different sampling periods Δ .

VII. CONCLUSIONS

In this paper, a framework for constraint handling of a generic nonlinear closed-loop system was described and demonstrated on a 5th-order hypersonic vehicle model. To provide the required closed-loop system, a feedback linearizing controller was designed with no knowledge of the system constraints. Two approaches were presented including the direct use of the nonlinear model and online linearizations of the model. In the first approach, sufficient conditions satisfying the assumptions required for theoretic results were presented. The plotted results demonstrate the effective enforcement of fuel-to-air ratio constraints using both approaches. However, the linearization-based approach may be more desirable for practical implementations as it does not suffer from the computational challenges and restrictive behaviour that the nonlinear approach exhibits.

REFERENCES

- [1] Z. T. Dydek, A. M. Annaswamy, and E. Lavretsky, "Adaptive control and the NASA X-15-3 flight revisited," *IEEE Control Systems Magazine*, vol. 30, no. 3, pp. 32–48, 2010.
- [2] J. W. Hicks, "Flight testing of airbreathing hypersonic vehicles," *National Aeronautics and Space Administration, Office of Management, Scientific and Technical Information Program*, 1993.
- [3] H. An, H. Xia, and C. Wang, "Barrier Lyapunov function-based adaptive control for hypersonic flight vehicles," *Nonlinear Dynamics*, vol. 88, no. 3, pp. 1833–1853, 2017.
- [4] X. Tao, N. Li, and S. Li, "Multiple model predictive control for large envelope flight of hypersonic vehicle systems," *Information Sciences*, vol. 328, pp. 115–126, 2016.

- [5] F. Borrelli, A. Bemporad, and M. Morari, *Predictive control for linear and hybrid systems*. Cambridge University Press, 2017.
- [6] E. G. Gilbert and I. Kolmanovsky, "Fast reference governors for systems with state and control constraints and disturbance inputs," *International Journal of Robust and Nonlinear Control: IFAC-Affiliated Journal*, vol. 9, no. 15, pp. 1117–1141, 1999.
- [7] A. Bemporad, A. Casavola, and E. Mosca, "Nonlinear control of constrained linear systems via predictive reference management," *IEEE Trans. on Automatic Control*, vol. 42, no. 3, pp. 340–349, 1997.
- [8] E. Gilbert and I. Kolmanovsky, "Nonlinear tracking control in the presence of state and control constraints: a generalized reference governor," *Automatica*, vol. 38, no. 12, pp. 2063–2073, 2002.
- [9] C. Petersen, M. Baldwin, and I. Kolmanovsky, "Model predictive control guidance with extended command governor inner-loop flight control for hypersonic vehicles," in *AIAA Guidance, Navigation, and Control (GNC) Conference*, 2013, p. 5028.
- [10] Q. Hu and Y. Meng, "Adaptive backstepping control for air-breathing hypersonic vehicle with actuator dynamics," *Aerospace Science and Technology*, vol. 67, pp. 412–421, 2017.
- [11] J. T. Parker, A. Serrani, S. Yurkovich, M. A. Bolender, and D. B. Doman, "Control-oriented modeling of an air-breathing hypersonic vehicle," *Journal of Guidance, Control, and Dynamics*, vol. 30, no. 3, pp. 856–869, 2007.
- [12] A. Isidori, E. Sontag, and M. Thoma, *Nonlinear control systems*. Springer, 1995, vol. 3.
- [13] D. Angeli, A. Casavola, and E. Mosca, "Command governors for constrained nonlinear systems: direct nonlinear vs. linearization-based strategies," *International Journal of Robust and Nonlinear Control: IFAC-Affiliated Journal*, vol. 9, no. 10, pp. 677–699, 1999.
- [14] G. C. Goodwin, S. F. Graebe, M. E. Salgado, *et al.*, *Control system design*. Prentice Hall New Jersey, 2001, vol. 240.

APPENDIX

Table I and II contain the system model parameters and the RG/CG design parameters. Since only longitudinal dynamics are considered the parameters m, I_{yy}, S, β_* should be interpreted as "per unit length" values.

TABLE I
SYSTEM MODEL AND MISCELLANEOUS PARAMETERS

m	3.0000×10^2 [lb-ft ⁻¹]	I_{yy}	5.0000×10^5 [lb-ft]
a_g	3.2174×10^1 [ft-s ⁻²]	S	1.7000×10^1 [ft]
\bar{c}	1.7000×10^1 [ft]	z^T	8.3600×10^0 [ft]
ρ_0	6.7429×10^{-5} [slugs-ft ⁻³]	ζ	7.0000×10^{-1} [-]
ω	2.0000×10^1 [rad-s ⁻¹]	C_1^L	4.6773×10^0 [rad ⁻¹]
C_1^L	-1.8714×10^{-2} [-]	C_2^D	5.8224×10^0 [rad ⁻²]
C_1^D	-4.5315×10^{-2} [rad ⁻¹]	C_0^D	1.0131×10^{-2} [-]
C_2^M	6.2926×10^0 [rad ⁻²]	C_1^M	2.1335×10^0 [rad ⁻¹]
C_e^M	-1.2897×10^0 [rad ⁻¹]	C_0^M	1.8979×10^{-1} [-]
β_1	-3.7693×10^5 [lb-ft ⁻¹ ·rad ⁻³]	β_2	-3.7225×10^4 [lb-ft ⁻¹ ·rad ⁻³]
β_3	2.6814×10^4 [lb-ft ⁻¹ ·rad ⁻²]	β_4	-1.7277×10^4 [lb-ft ⁻¹ ·rad ⁻²]
β_5	3.5542×10^4 [lb-ft ⁻¹ ·rad ⁻¹]	β_6	-2.4216×10^3 [lb-ft ⁻¹ ·rad ⁻¹]
β_7	6.3785×10^3 [lb-ft ⁻¹]	β_8	-1.0090×10^2 [lb-ft ⁻¹]

TABLE II
REFERENCE AND COMMAND GOVERNOR PARAMETERS

δ	1.0×10^{-5}	t_0	1.2×10^{-1} [s]
ϵ	1.0×10^{-4}	Δ	2.0×10^{-2} [s]
γ	1.0×10^{-1}	c_0	6
Ψ_μ	diag (10, 100, 300, 100, 10, 100, 100, 10)		
Ψ_w	diag (5, 50, 150, 50, 5, 50, 50, 5)		
Ψ_δ	diag (1, 10, 30, 10, 1, 10, 10, 1)		